Detailed diagnostics for a hot bromine plasma by the open *M*-shell opacity

Fengtao Jin and Jianmin Yuan*
Department of Physics, National University of Defense Technology, Changsha 410073, People's Republic of China
(Received 10 January 2005; revised manuscript received 9 May 2005; published 26 July 2005)

The experimental transmission spectrum of a hot bromine plasma [J. E. Bailey *et al.*, J. Quant. Spectrosc. Radiat. Transf. **81**, 31 (2003)] has been simulated by using a detailed level accounting model (DLA). With assumption of the local thermodynamic equilibrium, the major absorption lines of the experimental spectrum are well reproduced by the present DLA calculation, and the details of the absorption line shapes are used to determine the temperature of the plasma. In contrast to the results of two former statistical models, where the temperature was determined via a global fitting to the experimental data, the present DLA diagnoses the plasma temperature by the line ratios of different charge states in the $2p \rightarrow 3d$ transition groups resulting in a temperature of 37 eV. It is shown that a change of 1 eV in temperature could cause perceptible changes in the simulated spectrum. It is also shown that the $2p_{1/2} \rightarrow 3d_{3/2}$ absorptions have been overestimated by the statistical models.

DOI: 10.1103/PhysRevE.72.016404 PACS number(s): 52.25.Os, 52.20.−j

I. INTRODUCTION

Opacity dominates the radiative transfer within plasmas and consequently has strong influence on the radiative hydrodynamic evolutions. It is important for both astrophysical plasmas, as an example in the stellar envelopes, and laboratory plasmas, such as inertial confinement fusion (ICF) hohlraums. In addition, accurate opacity is prerequisite to many spectroscopic plasma diagnostics [1]. In the past decades, extensive studies on opacity have been done both experimentally and theoretically [1–18]. Among these works the opacities of medium-*Z* plasmas are of particular concern due to the practical needs as well as the challenge for theoretical simulations [1–12]. For theoretical simulations, opacity of medium-*Z* plasmas has sufficient complexity to be reasonably approximated by statistical techniques such as those using average atom (AA) or unresolved transition array (UTA) approaches, and also probably it can be treated by some detailed models such as the detailed term accounting (DTA) or the detailed level accounting (DLA) models. Medium-*Z* atoms with open *M*-shell configurations produce great complexities in atomic spectra. Although they are often concerned by the current opacity researches and involved in a variety of applications, few DTA/DLA works have been done until currently due to the great amount of computation and many uncertainties in the models. Experimental measurement of the medium-*Z* opacity provides benchmark data for the difficult theoretical simulations. Most recently a transmission spectrum of NaBr plasma has been measured by Bailey *et al.* [1] by using the *Z*-pinch radiation at the Sandia National Laboratories Z facility. The *L* to open *M* shell bromine absorptions were measured in a wide spectral range. Although some limitations still existed, this experiment, just as mentioned in Ref. [1], is an indication that opacity experiments with *Z*-pinch radiation heated samples are promising. Although many statistical methods have been developed for the treatments of the medium-*Z* plasmas, few detailed line models have been applied. The line-by-line calculations can reexamine the existing opacity data and help in the design of the future experiments. It is also important to use completely different computational methods to verify statistical approaches as they are employed for all elements over vast ranges of plasma conditions [6]. In the present study, the experimental transmission spectrum of the hot bromine plasma obtained by Bailey *et al.* [1] is simulated by using an independently developed DLA model simulation code. The massive atomic data are obtained by solving the full relativistic Dirac-Fock equation. Only configuration interaction (CI) within one configuration is considered to reduce the overly large scale matrixces of open *M*-shell configurations. With LTE assumption, the details of the absorption line shapes are used to determine the temperature of the plasma resulting in considerably different results from two former statistical models.

II. METHOD OF CALCULATION

Calculation of opacity requires a large number of atomic data, such as the atomic levels, level populations, oscillator strengths, transition line shapes, photoionization cross sections, free-free absorptions, and the photon scattering by free electrons. Details of the model were described in our previous paper [19], only the outline of the method is presented in the following.

In the case of the local thermodynamic equilibrium (LTE), the total absorption to a photon with energy $h\nu$ in a plasma is

$$\rho\kappa_\nu = \sum_i \left[\sum_{ll'} N_{il}\sigma_{ill'}(h\nu) + \sum_\alpha N_{i\alpha}\sigma_{i\alpha}(h\nu) + \mu_{ff}(h\nu) \right] \times (1 - e^{-h\nu/kT}) + \mu_s, \quad (1)$$

where κ_ν is the opacity at the energy $h\nu$, ρ the mass density of the plasma, T the temperature, $\sigma_{ill'}$ the cross section for the photoexcitation from level l to l' of ion i, σ_{ic} the total cross section for the photoionization from configuration α of

*Corresponding author. Email address: jmyuan@nudt.edu.cn

ion i, μ_{ff} the total free-free absorption coefficient, and μ_s the photon scattering cross section by free electrons. N_{il}, the population density for level l of ion stage i, is obtained from the Boltzmann distribution function

$$N_{il} = g_{il}(N_i/Z_i)e^{-E_{il}/kT}, \tag{2}$$

where g_{il} is the degeneracy of the state l. N_i, the total population density of ion i, is determined by solving the Saha equation [20]

$$\frac{N_{i+1}N_e}{N_i} = \frac{Z_{i+1}Z_e}{Z_i}\exp[-(\phi_i - \Delta\phi_i)/kT], \tag{3}$$

where N_e is the number of free electrons per unit volume, ϕ_i the ionization potential of ion i, and Z_i and Z_e the partition functions for ion i and free electron, respectively. In a plasma of high density, the energy levels of one atom will be perturbed by the neighboring ions and free electrons. In the present work, we take these effects into account as the so-called ionization potential depression (IPD), which will lower the ionization potential ϕ_i by $\Delta\phi_i$. The Stewart-Pyatt model [21] is used to evaluate the IPD. The bound-bound cross section for a given line can be expressed in terms of the oscillator strength $f_{ill'}$ and the line profile function as

$$\sigma_{ill'}(h\nu) = \frac{\pi he^2}{m_e c} f_{ill'} S(h\nu). \tag{4}$$

$S(h\nu)$ is taken to be in the Voigt form with the Doppler and Stark broadening considered. The Stark width was obtained from a simplified semiempirical method [22,23]. Rose's DCA [24] method was applied to account for the photoionization processes. The photoionization cross section of a configuration α of ion i is a weighted sum of all bound states that are explicitly considered

$$\sigma_{i\alpha}(h\nu) = \frac{\pi e^2}{m_e c} P_i(\alpha)\frac{df_{\alpha\to c}}{d(h\nu)}, \tag{5}$$

where $df_{\alpha\to c}/d\epsilon$ is the one-configuration photoionization oscillator density and $P_i(\alpha)$ is the relative occupation probability of configuration α calculated by Saha-Boltzmann equations. The Kramers [24] cross section was used to calculate the free-free absorptions and the Thompson scattering cross section was used to evaluate the scattering by free electrons.

In the experiment, people do not measure the opacity directly but the transmission instead. The relation between opacity and transmission is defined by

$$F(h\nu) = e^{-\rho\kappa(h\nu)L}, \tag{6}$$

where L is the path length traversed by the light through the plasma. The function F is integrated over a Gaussian function with the full width corresponding to the spectrometer resolution to obtain the final transmission spectrum.

In the calculation of the massive atomic data, the difficulties appear when the $3d$ orbital is nearly half filled. The number of the j-j coupling schemes becomes enormous even for one configuration. For example, the bound configuration $[\mathrm{Ne}]3s^2 3p^5 3d^5 4p$ of Br XIII has more than 20 000 of levels, and diagonalizing many CI matrixes with such a dimension is very time-consuming. In the present works, we parallelize the GRASP code [25] in the environment of the message passing interface (MPI), which is a set of standard code libraries supported by most of the current parallel computers. Linear efficiency with the number of computing nodes was found in our calculation.

III. RESULTS AND DISCUSSION

In the opacity calculation, accurate atomic energy levels and oscillator strengths are needed. We optimized the one-electron wave functions independently and obtained the energy levels by CI calculations within one configuration. Unfortunately, available experimental data for the energy levels of bromine are scarce, in particular, for some highly ionized ions such as Br X, Br XI, and Br XII. In Table I the calculated energy levels of some bromine ions are shown and compared with the existing experimental data [26]. For the ions listed in Table I, only a few low excited states are found in experimental data. Good agreements are found between the theory and experiments. Because of the scarcity of the experimental data for highly excited levels, we cannot make a direct comparison between theory and experiment, however, as discussed in the following paragraphs, the calculated transition energies are about 2 eV higher than the experimental data systematically.

We simulated the transmission spectrum [1] in the spectral range of 1450–1900 eV, which is dominated by the typical $n=2$ to $n=3$, 4, and 5 transitions. In the experiment [1], Bailey *et al.* measured the absorptions of the NaBr sample and took the Heδ and Heγ lines of the He-like sodium as the detector for the electron density, n_e, from the Stark broadening of the line shapes. An electron density of $3\pm1\times10^{21}$ cm^{-3} was determined by the best fits to the experimental data. According to the experimental conditions, we took $T=37$ eV and $\rho=0.025$ g/cm^3 in our calculation to best fit the measured spectrum in the $2p\to3d$ absorption groups. The calculated charge state distribution of bromine in the plasma is shown in Fig. 1 with an average charge state of 9.6. The total electron density is 2.38×10^{21} cm^{-3}, which is in the uncertainty range of the value provided by Bailey *et al.* Br X and Br XI are the main species in this case, which are 34.9% and 40.0% of the total number of the bromine ions, respectively.

Figure 2 shows the transmission calculated by using the present DLA model. Figure 2(a) is the transmission without convolution with the instrument response. Figure 2(b) is the spectrum convoluted with the spectrometer resolution. Figure 2(c) is a whole shift of Figure 2(b) downward by 2 eV to optimize the agreement with measurement. The features in the spectral range of 1480–1600 eV are the giant open M-shell absorptions, which are caused by the $2p\to3d$ transitions of the bromine ions. Because of the large splitting of the $2p$ orbitals, the $2p\to3d$ absorptions split into two groups. The absorptions around 1517 eV are from the $2p_{3/2}\to3d_{5/2}$ transitions and the absorptions around 1560 eV from the $2p_{1/2}\to3d_{3/2}$ transitions. In Fig. 3, the absorption lines of each ion are plotted in the $2p\to3d$ region and an artificial optical length is used in the calculation only to make it more illustrative. One can easily see that the $2p\to3d$ lines of the

TABLE I. Energy levels (in eV) of bromine atoms. Experimental data [26] are given for the comparison with the energy levels calculated by the relativistic one-configuration CI methods.

Ion	Configuration	Term	J	Calculated	Experiment
Br IV	$4s^24p^2$	^3P	0	0.000	0.000
			1	0.313	0.403
			2	0.709	0.773
		^1D	2	2.378	2.246
		^1S	0	5.024	4.769
	$4s^24p5p$	^3P	0	26.959	26.878
			1	27.235	27.210
			2	27.509	27.528
Br VI	$3d^{10}4s^2$	^1S	0	0.000	0.000
	$3d^{10}4s4p$	$^3P^o$	0	12.481	12.934
			1	12.751	13.196
			2	13.350	13.804
		$^1P^o$	1	20.205	18.756
	$3d^{10}4p^2$	^3P	0	30.210	30.269
			1	30.426	30.674
			2	30.021	31.479
	$3d^{10}4s4d$	^3D	1	37.492	37.772
			2	37.524	37.811
			3	37.569	37.871
Br VII	$3d^{10}4s$	^2S	1/2	0.000	0.000
	$3d^{10}4p$	$^2P^o$	1/2	15.741	15.904
			3/2	16.666	16.844
	$3d^{10}4d$	^2D	3/2	40.242	40.568
			5/2	40.036	40.675
Br IX	$3p^63d^9$	^2D	5/2	0.000	0.000
			3/2	1.108	1.066
	$3p^53d^{10}$	$^2P^o$	3/2	117.655	113.136
			1/2	124.766	119.310

bromine ions are strongly overlapped in this region. In the $2p_{3/2}\rightarrow 3d_{5/2}$ features, the transitions of each ion split into two groups, one is due to the transitions from the ground configuration and the other to the transitions from the excited configurations, i.e., the satellite lines. For example, the $2p_{3/2}\rightarrow 3d_{5/2}$ transitions from the ground configuration $[\mathrm{Ne}]3s^23p^63d^8$ of Br X contribute the absorptions around 1501 eV, and the transitions from excited configurations, such as $[\mathrm{Ne}]3s^23p^63d^7nl$ $(n=4,5,6,7)$, produce the main absorptions around 1517 eV. The transitions from the ground configuration of Br XII also have contributions near 1517 eV. The absorptions at 1509 eV arise from the transitions from the ground configuration of Br XI and the transitions from the excited configurations of Br IX. The absorptions at 1523 eV are mainly made by the transitions from the excited configurations of Br XI. Similarly, the experimental features caused by the $2p_{1/2}\rightarrow 3d_{3/2}$ absorptions can also be found in the calculations.

The identification of absorption lines is very important to the temperature diagnostic. Once the charge states having contributions to the spectrum are identified from the absorption lines, the plasma temperature can be determined by the

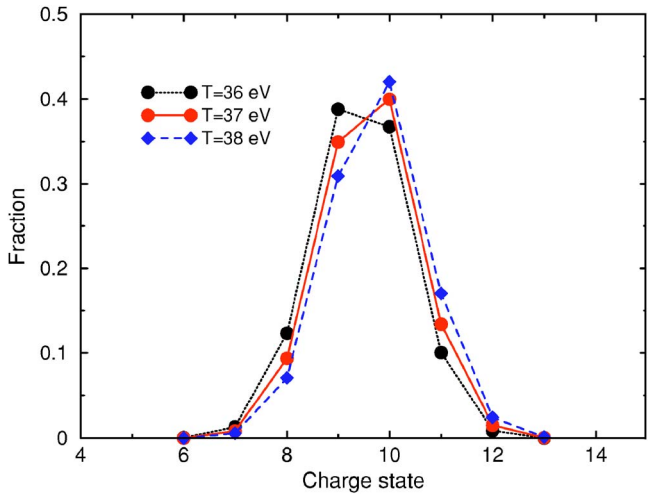

FIG. 1. (Color online) The charge state fractions in the bromine plasma at a density of 0.025 g/cm^3. The temperatures in the three cases are 36, 37, and 38 eV, respectively.

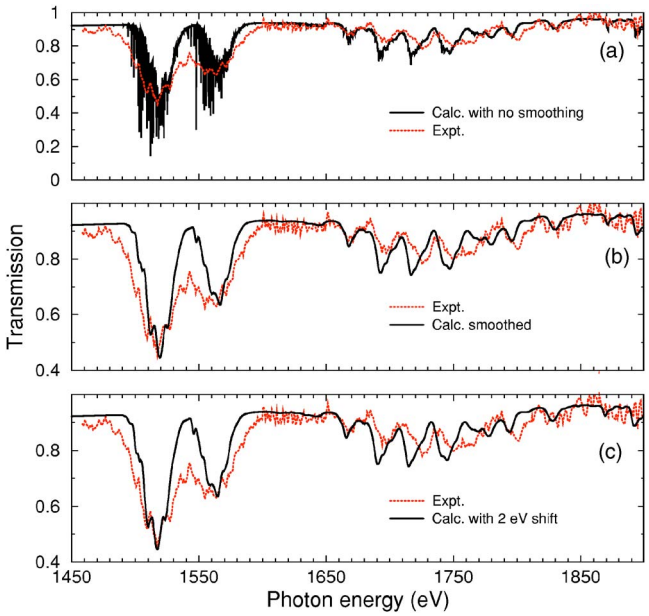

FIG. 2. (Color online) The radiative transmission of bromine plasma at a temperature of 37 eV and a density of 0.025 g/cm^3. The solid line in (a) refers to the theoretical results without convolution with spectral resolution and the dotted line refers to the experimental data. The solid line in (b) is the theoretical results, which are smoothed with a width of 1.4 eV according to the instrumental resolution in the experiment. The solid line in (c) is the same as that in (b) but having a 2 eV shift downward to fit the experimental data.

ratio of the absorption lines of different charge states. This is easily done for low-Z atoms but is rather difficult for medium-Z and high-Z atoms. In our previous paper [27], for an example, an aluminum transmission spectrum had been studied in the $1s \rightarrow 2p$ region, there were no overlapped lines between different charge states, and their contributions to the spectrum were clearly identified so that the plasma conditions could be easily determined. The difficulty in the temperature diagnostic of the bromine plasma is that the $2p \rightarrow 3d$ lines of the nearby charge states overlap considerably

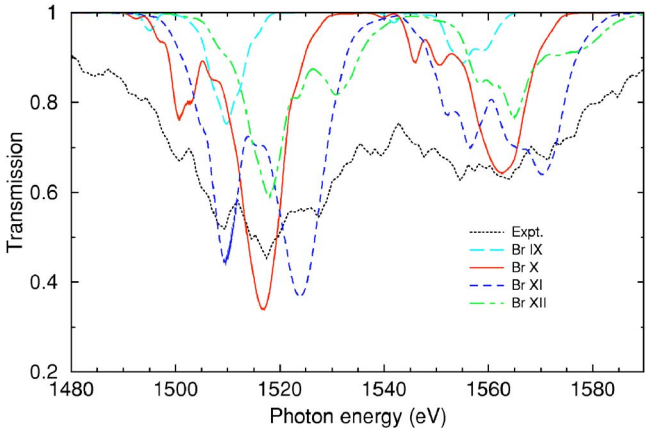

FIG. 3. (Color online) Absorption lines of bromine ions. An artificial optical length is used in calculation to make the figure more illustrative.

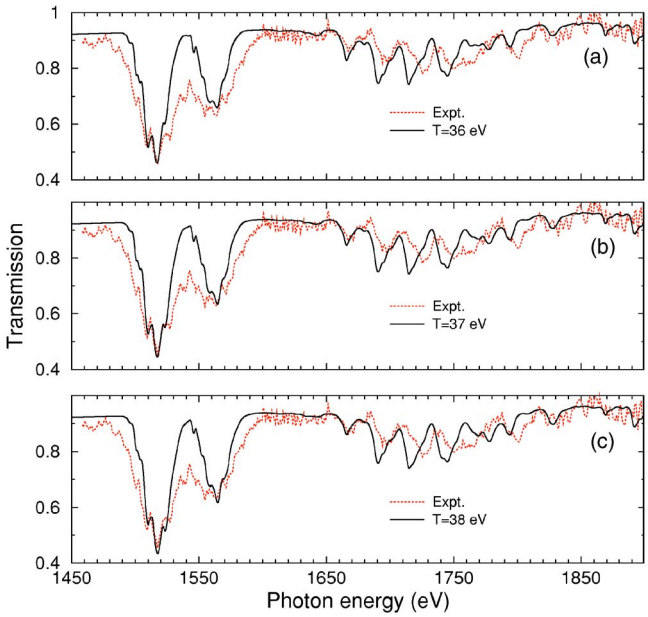

FIG. 4. (Color online) The temperature dependency of the spectrally resolved transmission at the density of 0.025 g/cm^3. The temperatures in (a), (b), and (c) are 36, 37, and 38 eV, respectively.

and that very accurate line positions and oscillator strengths are required in order to identify the experimental structures. The situation would get even worse if temperature and density nonuniformity exist in the plasma. In Fig. 3 one can easily see that the $2p \rightarrow 3d$ transition lines of the bromine ions overlap so strongly that they can only be identified from their transmission valleys. The separation between the $2p_{3/2} \rightarrow 3d_{5/2}$ lines of Br IX and Br X is about 8 eV, and the separation between the lines of Br X and Br XI is only about 6 eV. In theoretical calculations, errors of the line energy could lead to misinterpretations of the charge states. For an example, the absorption line at 1523 eV might be interpreted as the $2p_{3/2} \rightarrow 3d_{5/2}$ transition of Br X if the calculated line position is 6 eV higher than the actual one, and this would sequentially lead to a lower average charge state and a lower temperature. In Fig. 2(c) one can see that the DLA spectrum needs only a 2 eV shift downward to fit the experimental spectrum, and such a small shift would not lead to the misinterpretations of the charge states and the temperature.

Figure 4 shows the temperature dependency of the spectrally resolved transmission at the density of 0.025 g/cm^3. In a plasma, the absorption strengths of a charge state depend on its population fraction. In Fig. 4(a), the calculated absorptions around 1523 and 1564 eV are weaker than the experimental data while the calculated absorptions around 1509 eV are stronger. We have mentioned that the absorptions nearby 1523 eV are from the $2p_{3/2} \rightarrow 3d_{5/2}$ transitions of Br XI and that the absorptions nearby 1509 eV are from Br XI and Br IX. Stronger absorptions around 1523 eV require a higher temperature of the plasma with a higher population of Br XI. Although the absorptions of Br XI around 1509 eV increase also with the increase of its population, the contribution of Br IX decrease much more and the total absorptions around 1509 eV decrease as well along with the increase of the temperature of the plasma. Figure 4(b) shows the best fit for the

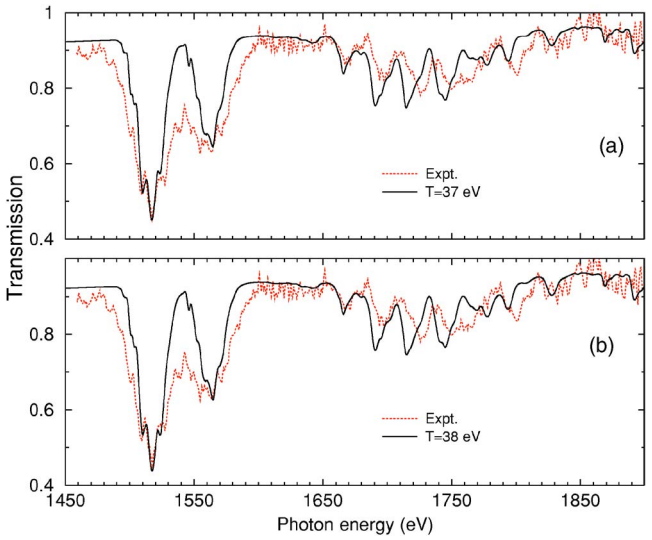

FIG. 5. (Color online) Calculated transmission at the density of 0.03 g/cm^3. The temperatures in (a) and (b) are 37 and 38 eV, respectively.

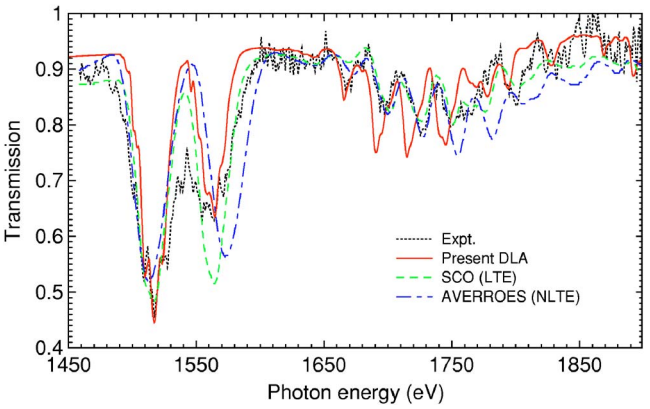

FIG. 6. (Color online) Comparison among the theoretical results and experimental data. Dotted line refers to experimental data, solid line refers to our DLA model, dashed line refers to the result of a LTE code SCO [1], and dot-dashed line refers to the result of a NLTE code AVERROES [1].

experimental data when the temperature is chosen to be 37 eV. In Fig. 4(b), both the line ratios within the $2p_{3/2} \rightarrow 3d_{5/2}$ transition group and the ratio between the two $2p \rightarrow 3d$ groups have good agreements with experiment. When the temperature increases to 38 eV, the absorption at 1523 eV becomes stronger than the experimental data while absorptions at 1509 eV are reduced to be smaller. It seems that the calculated results with $T=38$ eV are overionized compared with the experiment. From Figs. 4(a)–4(c), one can see that a change of 1 eV in temperature can cause perceptible changes in the simulated spectrum, in particular for the relative strength of the absorption structures between 1500 and 1530 eV.

Nevertheless, the structures of the transmission spectrum depend also on the density. Figure 5 shows the calculated spectra at a plasma density of 0.03 g/cm^3 with two temperatures of 37 and 38 eV. The electron densities are 2.86×10^{21} and 2.81×10^{21} cm^{-3}, respectively. Compared with the spectra at $\rho=0.025$ g/cm^3, slight differences appear nearby 1509 and 1523 eV. With this density, the experimental transmission spectrum could be reproduced well by taking the temperature between 37 and 38 eV. After a thorough calculation of the opacity by changing the electron density within the uncertainty range given by Bailey *et al.*, the plasma temperature has been changed no more than 1 eV from 37 eV in order to reproduce the measured spectrum. That is to say the temperature should be 37 ± 1 eV for the electron densities $3\pm1\times10^{21}$ cm^{-1}. In contrast to the ±30% uncertainty of the electron density, a relatively small deviation is found for the temperature. Because of the fact that strong line overlaps exist in the $2p \rightarrow 3d$ transition groups and of the limited experimental spectral resolution, the present DLA calculation could not give more accurate diagnostics for both temperature and density at the same time.

Despite the impressive agreements, differences still exist for the strengths of the $n=2-4$ transition groups from 1528 to 1550 eV. Absorptions in this spectral range are observed in the experimental spectrum much more strongly than the theoretical simulation. It indicates that the Br XII, Br XIII, and Br XIV ions should have larger population fractions than the theoretical predictions. Although the DLA spectrum in Fig. 3 has some lines between 1528 and 1550 eV, they are too weak to reproduce the measured data. One of the possible reasons for this discrepancy is the temperature gradient in the experimental sample. Absorptions with higher temperatures might be mixed in the final spectrum and then the measured $2p \rightarrow 3d$ structures appear having a larger width than the calculations. Another source is probably the spatial nonuniformity of the plasma conditions.

In Fig. 6, the transmissions calculated by the present DLA model, two other statistical models, and the experimental spectrum are plotted together for comparison. The dotted line refers to the result of the SCO code [1], which is a superconfiguration transition array model in the approximation of LTE. The SCO calculation was performed at the electron temperature of 45 eV and the electron density of 3×10^{21} cm^{-3}. The dot-dashed line refers to a NLTE code AVERROES, which is also a superconfiguration model. The AVERROES calculation was performed at $T_e=49$ eV and $n_e=3\times10^{21}$ cm^{-3}. The temperatures used in the SCO and AVERROES calculations are rather larger than the present DLA calculation. The SCO spectrum has been shifted downward by about 23 eV [1]. There are considerable discrepancies between the statistical models and the present DLA for the main structures from 1450 to 1600 eV, in particular for the relative strength between the absorptions around 1519 and around 1560 eV. The differences between the statistical models and the present DLA are mainly due to the higher temperatures and the different treatments of the atomic processes taken in the statistical models.

In Fig. 6, both the positions and the strengths of the SCO calculation agree well with experiment for the $2p_{3/2} \rightarrow 3d_{5/2}$ and the $2p \rightarrow 4d$ transition arrays. However, the relative strength between the $2p_{3/2} \rightarrow 3d_{5/2}$ and $2p_{1/2} \rightarrow 3d_{3/2}$ transition arrays is apparently different from the experiment. The same situation appears in the AVERROES result. Further more, the splitting between the $2p_{3/2} \rightarrow 3d_{5/2}$ and the $2p_{1/2} \rightarrow 3d_{3/2}$

transition arrays appears too large. In contrast to the two statistical models, the present DLA calculation has quite good agreements for both the line positions and the relative strength for the $2p \rightarrow 3d$ transition groups. Model deficiency is the possible reason of the incorrect line ratio in the two statistical models. The line ratio is defined by the electronic populations in $2p_{1/2}$ and $2p_{3/2}$ orbitals as well as the $2p_{1/2} \rightarrow 3d_{3/2}$ and $2p_{3/2} \rightarrow 3d_{5/2}$ oscillator strengths. Since $2p_{1/2}$ and $2p_{3/2}$ orbitals are almost full at the calculation conditions, the possible reason is that the $2p_{1/2} \rightarrow 3d_{3/2}$ oscillator strengths may be overevaluated by the statistical models. In all the theoretical calculations, the strong absorptions in the spectral range of 1528–1550 eV observed in the experimental data for the transitions of Br XII–XIV are not well reproduced. The measured spectrum showed a broader distribution of the charge states and wider absorption structures than the theoretical predictions. This discrepancy between theory and experiment is most likely due to the temperature gradient and the spatial nonuniformity of the plasma sample, which have not been taken into account in all theoretical simulations. Another difference between the present and the other two simulations worthy of note is that the DLA determines the temperature by using the detailed structures in the $2p \rightarrow 3d$ transition array nearby 1519 eV while the SCO and AVERROES obtain their temperatures by the best fit of the global structures of the experimental spectrum. For an experimental spectrum with well resolved lines, the DLA model can give more accurate temperature and density information.

We also carry out a calculation for the temperature of 45 eV and the density of 0.025 g/cm^3. The average charge state is 10.9, which is very close to the value obtaind in the SCO calculation [1]. The main species in the plasma are Br XI, Br XII, and Br XIII, which are 28.6%, 36.1%, and 23.0% of the total, respectively. In Fig. 7(a), the calculated transmission spectrum are plotted. One can see that the positions of the $2p \rightarrow 3d$ transitions are predicted much higher than the experiment. After a 10 eV shift downward, the spectrum agree with experiment in the spectral range of the $2p \rightarrow 3d$ absorptions, but the discrepancies in the $2p \rightarrow 4d$ absorptions get even worse than in the case of $T=37$ eV. In addition, the detailed structures in the $2p_{3/2} \rightarrow 3d_{5/2}$ transition array are not as good as those in the case of $T=37$ eV either.

In summary, we simulate a bromine spectrum [1] by using a detailed level accounting model. The calculated $n=2$ to 3, 4, 5 absorptions have good agreements with experimental data. However, the measured $2p \rightarrow 3d$ absorptions spread in a wider spectral range than the theoretical predictions. Although the diagnostic of the plasma conditions for medium-Z plasma is rather difficult and complex, because of the strong overlap between the transition lines, it is possible to obtain the temperature of the plasma by comparing the details of the absorption structures between theory and experiment. It also suggests that a higher spectral resolution experiment of medium-Z opacity would be very helpful for both theory and the plasma diagnostics. The difference between theory and experiment shows that temperature gradient probably exists in the measurement. Comparisons are also performed between the present DLA model and two statistical models. It shows that the $2p_{1/2} \rightarrow 3d_{3/2}$ oscillator strengths might be overevaluated by the SCO and AVERROES codes. Different diagnostic references result in a quite different temperature of the plasma from the statistical models.

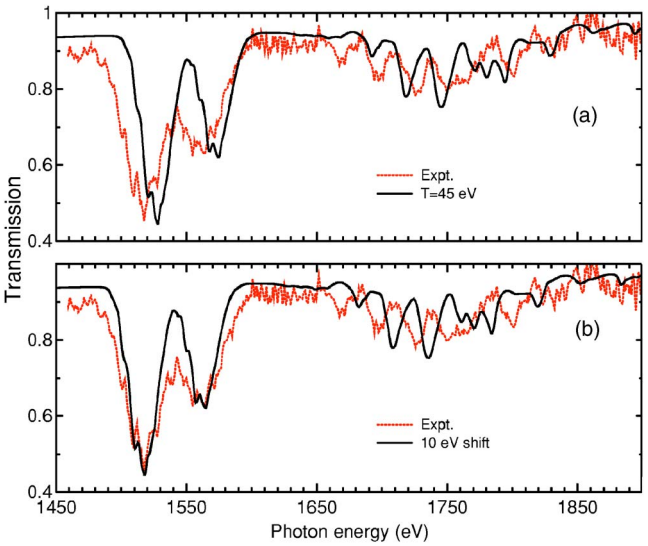

FIG. 7. (Color online) The DLA spectrum at a temperature of 45 eV and a density of 0.025 g/cm^3. The theoretical spectrum in (b) has been shifted 10 eV downward to fit the $2p \rightarrow 3d$ lines.

ACKNOWLEDGMENTS

This work was supported by the National Science Fund for Distinguished Young Scholars under Grant No. 10025416, the National Natural Science Foundation of China under Grant No. 10474138, the National High-Tech ICF Committee in China, and the China Research Association of Atomic and Molecular Data.

[1] J. E. Bailey, P. Arnault, T. Blenski, G. Dejonghe, O. Peyrusse, J. J. MacFarlane, R. C. Mancini, M. E. Cuneo, D. S. Nielsen, and G. A. Rochau, J. Quant. Spectrosc. Radiat. Transf. **81**, 31 (2003).
[2] J. E. Bailey *et al.*, Phys. Plasmas **9**, 2186 (2002).
[3] P. T. Springer *et al.*, Phys. Rev. Lett. **69**, 3735 (1992).
[4] P. T. Springer *et al.*, J. Quant. Spectrosc. Radiat. Transf. **51**, 371 (1994).
[5] P. T. Springer *et al.*, J. Quant. Spectrosc. Radiat. Transf. **58**, 927 (1997).
[6] C. A. Iglesias, M. H. Chen, V. Sonnad, and B. G. Wilson, J. Quant. Spectrosc. Radiat. Transf. **81**, 227 (2003).
[7] T. S. Perry *et al.*, Phys. Rev. Lett. **67**, 3784 (1991).
[8] T. S. Perry *et al.*, Phys. Rev. E **54**, 5617 (1996).
[9] M. E. Foord, S. H. Glenzer, R. S. Thoe, K. L. Wong, K. B. Fournier, B. G. Wilson, and P. T. Springer, Phys. Rev. Lett. **85**,

992 (2000).
[10] M. E. Foord *et al.*, Phys. Rev. Lett. **93**, 055002 (2004).
[11] K. L. Wong, M. J. May, P. Beiersdorfer, K. B. Fournier, B. Wilson, G. V. Brown, and P. T. Springer, Phys. Rev. Lett. **90**, 235001 (2003).
[12] F. J. D. Serduke, E. Minguez, S. J. Davidson, and C. A. Iglesias, J. Quant. Spectrosc. Radiat. Transf. **54**, 437 (1995).
[13] G. Winhart, K. Eidmann, C. A. Iglesias, A. Bar-Shalom, E. Minguez, A. Rickert, and S. J. Rose, J. Quant. Spectrosc. Radiat. Transf. **54**, 437 (1995).
[14] G. Winhart, K. Eidmann, C. A. Iglesias, and A. Bar-Shalom, Phys. Rev. E **53**, R1332 (1996).
[15] M. J. Seaton, J. Phys. B **20**, 6363 (1987).
[16] D. G. Hummer, K. A. Berrington, W. Eissner, A. K. P. H. E. Saraph, and J. A. Tully, Astron. Astrophys. **279**, 298 (1993).
[17] F. J. D. Serduke, E. Minguez, Steven J. Davidson, and C. A. Iglesias, Astrophys. J. **144**, 1203 (1966).
[18] L. B. DaSilva, B. J. MacGowan, D. R. Kania, B. A. Hammel, C. A. Back, E. Hsieh, R. Doyas, C. A. Iglesias, F. J. Rogers, and R. W. Lee, Phys. Rev. Lett. **69**, 438 (1992).
[19] F. Jin, J. Zeng, and J. Yuan, Phys. Rev. E **68**, 066401 (2003).
[20] X. S. Xu, *Introduction to Practical Theory of EOS* (Science Press, Bejing, China, 1986) (in Chinese).
[21] J. C. Stewart and K. D. Pyatt, Jr., Astrophys. J. **144**, 1203 (1966).
[22] M. S. Dimitrijevic and N. Konjevic, J. Quant. Spectrosc. Radiat. Transf. **24**, 451 (1980).
[23] M. S. Dimitrijevic and N. Konjevic, Astron. Astrophys. **172**, 345 (1987).
[24] S. J. Rose, J. Phys. B **25**, 1667 (1992).
[25] F. A. Parpia, C. F. Fischer, and I. P. Grant, Comput. Phys. Commun. **94**, 249 (1996).
[26] R. L. Kelly, J. Phys. Chem. Ref. Data **16**, Suppl. N1 (1987).
[27] J. Zeng, F. Jin, J. Yuan, and Q. Lu, Phys. Rev. E **62**, 7251 (2000).